DOI10.1002/aic.16625

Rational design of double salt ionic liquids as extraction solvents: Separation of thiophene/*n*-octane as example

Zhen Song[a], Xutao Hu[b], Yageng Zhou[a], Teng Zhou[a,*], Zhiwen Qi[b], Kai Sundmacher[a,c]

[a] *Process Systems Engineering, Max Planck Institute for Dynamics of Complex Technical Systems, Sandtorstr. 1, D-39106 Magdeburg, Germany*

[b] *Max Planck Partner Group at the State Key Laboratory of Chemical Engineering, School of Chemical Engineering, East China University of Science and Technology, 200237 Shanghai, China*

[c] *Process Systems Engineering, Otto-von-Guericke University Magdeburg, Universitätsplatz 2, D-39106 Magdeburg, Germany*

* *Corresponding author:* zhout@mpi-magdeburg.mpg.de (Teng Zhou)

Abstract

Although double salt ionic liquids (DSILs) offer significant advantages over classical two-ion ionic liquids (ILs) as separation solvents, relevant studies are still scarce and a systematic DSIL selection method is thus highly desirable. In this contribution, a rational method for designing DSILs as extraction solvents is proposed and exemplified by the thiophene/*n*-octane separation. The effects of additional degrees of freedom for DSIL design (i.e., double cations and/or anions and the ion ratio) on the thermodynamic properties are first analyzed by COSMO-RS. Then, a multilevel DSIL design method combining the prediction of infinite dilution thermodynamic properties, the estimation of physical properties, the evaluation of phase equilibrium behavior, and the experimental validation is proposed. By applying this method, $[C_2MIm][OAc]_x[NO_3]_{1-x}$

This article has been accepted for publication and undergone full peer review but has not been through the copyediting, typesetting, pagination and proofreading process which may lead to differences between this version and the Version of Record. Please cite this article as doi: 10.1002/aic.16625

Received: May 21, 2018;Revised: Mar 04, 2019;Accepted: Apr 29, 2019

(x=[0, 1]) and $[C_2MIm][OAc]_x[SCN]_{1-x}$ (x=[0.70, 1]) are identified as promising DSIL solvents for the thiophene/*n*-octane separation. Correspondingly, the liquid-liquid equilibria of {DSILs + thiophene + *n*-octane} with the designed DSILs are experimentally studied.

Keywords: double salt ionic liquids; solvent design; COSMO-RS; thiophene/*n*-octane separation; liquid-liquid equilibrium

Introduction

During the past decades, ionic liquids (ILs) have sparked significant interest for application in various separation processes due to their overwhelming advantages over conventional organic solvents, such as negligible vapor pressure, broad liquid range, designable and tunable character, and so on.[1-10] However, as known to all, various cation-anion combinations can lead to very different physical and thermodynamic properties, making the selection of ILs the most crucial task for the development of IL-based separation processes.[4-10]

A large number of experimental and theoretical studies have been reported on the identification of suitable ILs for different separation processes.[7-25] Particularly, several research groups have employed COSMO-based activity coefficient models[12-19] or the UNIFAC-IL model[20-25] to perform computational screening and design of ILs as separation solvents. Because of the predictive character of these thermodynamic models, the separation performance of ILs that have not been experimentally covered can be estimated and thus the identification of suitable solvent

candidates in a large range is possible. Despite the progress made, the selection of practically attractive IL for a specific process is still challenging since in many cases very few ILs can satisfy different desirable properties simultaneously. For instance, when screening ILs as extractive desulfurization solvent, Song et al. found that only 831 of the initial 36260 cation-anion combinations meet the thermodynamic property requirements, among which only 15 satisfy the physical property constraints.[16] Conceivably, if more restrictions such as easy preparation, commercial availability, low cost, etc. of ILs are considered, the number of feasible solvents will be further reduced and in some cases even no candidates could retain. This problem represents a major obstacle in the practical application of ILs for separation processes.[11,17,26] Nevertheless, it should be noted that most of the previous studies focused on classical two-ion (i.e., one cation and one anion) ILs only.

Moving beyond two-ion ILs, several researchers have recently turned their attention to double salt ionic liquids (DSILs) which are composed of more than one cation and/or anion.[27-37] Since the most straightforward approach to obtain such DSILs is mixing two different ILs together, they are treated as 'IL mixtures' in many studies (in the following all ILs refer to two-ion ones if they are not particularly specified).[27-31] However, through an elaborate review, Rogers and co-workers suggested the concept of DSILs since they found that the 'mixture' of ILs is quite different from the mixture of molecular solvents: (a) the ionic associations in the individual ILs are lost and one cannot identify which ion is from which IL; (b) the overall properties of the

'mixture' are derived from the ion identities and ion ratios in it, not necessarily derived from the individual ILs (also named as IL parents of DSIL) used for its preparation.[37]

No matter how DSILs are called, they are generally recognized to have two notable advantages over two-ion ILs. First, DSILs significantly extend the solvent selection space.[31,32,37] It is estimated that the maximal number of possible two-ion ILs are around 10^6, and so far only a few hundreds of them have been commercialized or experimentally synthesized. In contrast, the number of DSILs resulting from the combinations of two-ion ILs is many orders of magnitude larger. Even if the commercialized or experimentally synthesized ILs are considered only, a huge space of DSILs can still be achieved. Second, DSILs offer an easy approach to tune solvent properties.[32,37] Normally, the properties of two-ion ILs are tailored by altering functional groups and/or alkyl chains; however, the synthesis and purification of the resultant ILs, in some cases functional ILs, are always complex, which may greatly limit their interests from application point of view. By comparison, by changing the identities or the ratios of IL parents for DSIL preparation, the physical and thermodynamic properties of the obtained solvent can be readily tuned in a wide range. For instance, Pinto et al. observed that the viscosity of the 'mixture' of $[C_2MIm][NTf_2]$ and $[C_4EIm][EtSO_4]$ varies from 32.6 mPa·S to 255.2 mPa·S with the molar fraction of $[C_4EIm][EtSO_4]$ increasing from 0 to 1;[30] Lei et al. found that the solubility of CO_2 in the 'mixture' of $[C_8MIm][NTf_2]$ and $[C_nMIm][BF_4]$ (n=2, 4) can be adjusted by different IL compositions.[28] For these reasons, DSILs open new horizons for the identification of suitable solvents for separation processes. However, compared to the extensive studies on two-ion ILs,

the ones on DSILs are still very scarce, among which the ideal or non-ideal 'mixture' behaviors of DSILs are mainly concentrated on.[32,37-40] To the best of our knowledge, until now, there is no systematic study on the optimal selection of DSILs for separation tasks.

In the present work, the rational design of DSILs as extraction solvents is investigated, where the separation of the mixture thiophene/*n*-octane, a typical fuel oil model in extractive desulfurization studies, is applied as an illustrative example. First, the effects of introducing double cations and/or anions as well as the effect of different ion ratios on the thermodynamic properties of DSILs are evaluated in order to identify key degrees of freedom for DSIL design. Following this, a multilevel DSIL design method is proposed and further applied to the thiophene/*n*-octane separation. The practical separation performances of the designed DSILs are finally validated by liquid-liquid equilibrium (LLE) experiments.

Evaluation of key degrees of freedom for DSILs design

Among the different types of DSILs summarized by Chatel et al.,[37] namely $[C_1]_x[C_2]_{1-x}A$, $C[A_1]_x[A_2]_{1-x}$, $[C_1A_1]_x[C_2A_2]_{1-x}$, $[C_1]_x[C_2]_y[C_3]_{1-x-y}A$, $C[A_1]_x[A_2]_y[A_3]_{1-x-y}$, and $[C_1^{i}]_{x/i}[C_2^{ii}]_{(1-x)/ii}[A_1^{iii}]_{y/iii}[A_2^{iv}]_{(1-y)/iv}$, the first three are more applicable from practical point of view since they can be easily prepared by mixing two ILs together (C and A represent cation and anion, respectively; *x* and *y* refer to the molar ion ratio; *i*, *ii*, *iii*, and *iv* denote valence of ions). Comparing these three types of DSILs to classical two-ion ILs, one more cation and/or anion, as well as the ion ratio are introduced as additional degrees of freedom. Therefore, before proposing the method to design such DSILs, the effects of these novel degrees of freedom on their

thermodynamic properties are evaluated. For this purpose, in the example of thiophene/*n*-octane separation, the infinite dilution capacity and selectivity of different DSILs, i.e., C^{∞} and S^{∞}, are calculated by COSMO-RS as follows:

$$C^{\infty} = 1/\gamma^{\infty}_{\text{thiophene}} \quad (1)$$

$$S^{\infty} = \gamma^{\infty}_{\text{octane}}/\gamma^{\infty}_{\text{thiophene}} \quad (2)$$

where $\gamma^{\infty}_{\text{thiophene}}$ and $\gamma^{\infty}_{\text{octane}}$ stand for the infinite dilution activity coefficient of thiophene and *n*-octane in DSILs, respectively. The C^{∞} and S^{∞} can offer a simple and quick estimation of the separation performances of DSILs for the extraction of thiophene from *n*-octane.[12,16] In the calculation, 20 common cations of the imidazolium, pyridinium, and pyrrodinium families are covered together with 25 widely reported anions. Their detailed information is provided in Table S1 (Supporting Information). An elaborate introduction of the COSMO-RS model and its applications in calculating different thermodynamic properties can be found in literature.[41] It has been widely demonstrated to be able to provide good qualitative and in many cases acceptable quantitative predictions on the thermodynamic properties of IL-involved systems,[42-48] and is thus also promising for estimating the separation performances of DSILs.[29,31,49]

It should be noted that in COSMO-RS calculations ILs including DSILs are treated as electroneutral mixtures of dissociated cations and anions with the molar ratio corresponding to the stoichiometry, whereas in the experimental context they are normally treated as one compound. Therefore, as demonstrated in the COSMOthermX manual (Version C3.0, Release 16.01), COSMO-RS derived properties that depend on the definition of mole fraction, such as

the infinite dilution activity coefficients in Eqs. 1-2, have to be converted to ensure the same reference standard as used in experiments.

Effect of introducing double cations and/or anions

When analyzing the effect of double cations and/or anions, the ion ratios in DSILs are fixed at 0.5. Based on the involved 20 cations and 25 anions, there are totally 4750 $[C_1]_{0.5}[C_2]_{0.5}A$ and 6000 $C[A_1]_{0.5}[A_2]_{0.5}$ DSILs. To avoid the combinatorial explosion, a reduced set of 10 cations and 20 anions (marked in Table S1, Supporting Information) are considered in the $[C_1A_1]_{0.5}[C_2A_2]_{0.5}$ case, which results in 8550 DSILs of this type. The calculated C^{∞} and S^{∞} of these DSILs are tabulated in Table S2 (Supporting Information), together with those of the 500 two-ion ILs based on the same set of cations and anions.

Figures 1 and 2 show the effect of introducing double cations or anions on the C^{∞} and S^{∞} of DSILs with the examples of $[C_4MIm]_{0.5}[Cation]_{0.5}[BF_4]$ and $[C_4MIm][BF_4]_{0.5}[Anion]_{0.5}$. As seen in Figure 1, with the variation of the second cation in the $[C_4MIm]_{0.5}[Cation]_{0.5}[BF_4]$ DSILs, the C^{∞} and S^{∞} of them change in a large range and generally follow a reverse trend along the *x* axis. For instance, when introducing $[C_2MIm]^+$, $[C_6MIm]^+$, $[C_8MIm]^+$, and $[C_{10}MIm]^+$ into $[C_4MIm]_{0.5}[Cation]_{0.5}[BF_4]$, the C^{∞} of the obtained DSILs are 0.56, 0.66, 0.72, and 0.79 while their S^{∞} are 327.30, 136.72, 94.88, and 67.52, respectively. Such a reverse trend of the notably changing C^{∞} and S^{∞} can also be roughly observed as the anion changes along the *x* axis in the example of $[C_4MIm][BF_4]_{0.5}[Anion]_{0.5}$ (see Figure 2). These results demonstrate that introducing different cations or anions into DSILs is an effective approach to adjust and balance their C^{∞} and

S^{∞}. Interestingly, the C^{∞} and S^{∞} of $[C_4MIm]_{0.5}[Cation]_{0.5}[BF_4]$ can be positively correlated to those of the corresponding two-ion ILs $[Cation][BF_4]$; this also holds true when comparing the C^{∞} and S^{∞} of $[C_4MIm][BF_4]_{0.5}[Anion]_{0.5}$ with those of $[C_4MIm][Anion]$ (see Figure S1, Supporting Information). These findings suggest that one can roughly tune the C^{∞} and S^{∞} of $[C_4MIm]_{0.5}[Cation]_{0.5}[BF_4]$ and $[C_4MIm][BF_4]_{0.5}[Anion]_{0.5}$ DSILs according to the knowledge on their IL parents, i.e., $[Cation][BF_4]$ and $[C_4MIm][Anion]$.

From Figures 1 and 2, it can be inferred that the introduction of a second cation-anion combination will also have a remarkable effect on the C^{∞} and S^{∞} of the $[C_1A_1]_{0.5}[C_2A_2]_{0.5}$ DSILs (see Table S2c, Supporting Information). Overall, different identities of cation, anion, and cation-anion combination introduced in DSILs are important degrees of freedom for DSIL design.

Effect of ion ratio

To evaluate the effect of ion ratio (x) of DSILs on their separation performances, the C^{∞} and S^{∞} of $[C_1]_x[C_2]_{1-x}A$, $C[A_1]_x[A_2]_{1-x}$, and $[C_1A_1]_x[C_2A_2]_{1-x}$ with varying x from 0 to 1 are predicted. According to the COSMO-RS results, the involved DSILs can be classified into three groups based on the different dependencies of their C^{∞} on x (see Figure 3 for the representative DSILs of each type). For DSILs in Group 1, their C^{∞} change monotonically between those of their IL parents; for DSILs in Group 2 and Group 3, their C^{∞} vary parabolically, showing a minimum and a maximum value at a certain ion ratio, respectively. The number of DSILs in each group is summarized in Table 1 with their detailed information tabulated in Table S3 (Supporting Information). As seen, the majority of DSILs belongs to Group 1, accounting for 90.8%, 83.8%,

and 78.4% of the total number of $[C_1]_x[C_2]_{1-x}A$, $C[A_1]_x[A_2]_{1-x}$, and $[C_1A_1]_x[C_2A_2]_{1-x}$, respectively. In addition, a notable number of DSILs fall into Group 2 while very few DSILs are found in Group 3. It is clear that the dependencies of C^∞ for DSILs in Group 2 and Group 3 indicate strong non-ideal 'mixing' behaviors of their IL parents; even for DSILs in Group 1, their C^∞ may deviate noticeably from that averaged for their IL parents. Very recently, such distinct effects of *x* were also observed on the solubility of DSILs for paracetamol and CO_2, where the different 'mixing' performances of DSILs were understood by means of the σ-profiles of involved molecules and the thermodynamic analysis of DSIL solvents.[31,40] A similar interpretation for the different dependencies of C^∞ of DSILs for thiophene on *x* is illustrated in Figures S2 - S3 (Supporting Information) with the representative $C[A_1]_x[A_2]_{1-x}$ DSILs.

The S^∞ of DSILs in different groups also vary remarkably with increasing *x*, but their dependencies seem to be not related to those of C^∞. For instance, as shown in Figure 3, a monotonic increase or decrease is observed for the S^∞ of the representative DSILs of Group 1 and Group 3, although their C^∞ change in different trends. For the representative DSILs of Group 2, their S^∞ may have distinct dependencies on *x*, such as the monotonic decrease of S^∞ for $[C_4MIm][OAc]_x[Tf_2N]_{1-x}$, and the parabolic evolution of S^∞ for $[C_3MPyr]_x[C_8MPy]_{1-x}[MeSO_4]$ and $\{[C_2MIm][NO_3]\}_x\{[C_7MIm][B(CN)_4]\}_{1-x}$. The irregular dependencies of the S^∞ of DSILs on *x* could be attributed to the fact that it is a quotient property between $\gamma^\infty_{\text{octane}}$ and $\gamma^\infty_{\text{thiophene}}$ of DSILs (as defined in Eq. 2).

To summarize, the ion ratio of DSILs has a significant effect on their C^{∞} and S^{∞}, and thus should also be considered as an important degree of freedom for DSIL design. Moreover, the C^{∞} and S^{∞} of DSILs are generally non-ideal 'mixing' properties of their IL parents since they always deviate from the correspondingly parent-averaged values to different extents. In order to screen suitable DSILs for a specific application, one should first identify the Group of the interesting candidates. For DSILs of Group 1, only the IL parents with high C^{∞} and/or S^{∞} are worth to be studied since changing the ion ratio only allows a trade-off between the two parameters. In contrast, for DSILs belonging to Group 2 and 3, the ion ratios should be optimized to determine the optimal DSIL.

Description of the DSILs design method

As discussed above, each unique combination of ion identities and ion ratios may constitute a unique DSIL with specific properties. In other words, even two small sets of cations and anions can give rise to a huge number of possible DSILs, making the experimental trial-and-error method unrealistic for DSIL design. Moreover, besides the C^{∞} and S^{∞} of DSILs, their physical and thermodynamic properties at specific conditions of interest should also be evaluated in order to identify practically attractive extraction solvents.[16,25] In this context, a systematic DSIL design method is proposed as illustrated in Figure 4, which consists of four steps. The first three model-based steps are employed to screen promising DSILs candidates from an enormous number of combinations of ion identities and ion ratios by setting constraints on their thermodynamic and

physical properties. The fourth step is the experimental determination of the liquid-liquid equilibria (LLE) of the systems composed of the screened DSILs and the target mixture to be separated, thereby finally identifying the optimal DSIL solvent. In the following, the proposed method is introduced with the example of thiophene/*n*-octane separation.

COSMO-RS based prediction of infinite dilution thermodynamic properties

In the first step, the same set of DSILs as introduced in Section 2.1, i.e., 4750 $[C_1]_{0.5}[C_2]_{0.5}A$, 6000 $C[A_1]_{0.5}[A_2]_{0.5}$, and 8550 $[C_1A_1]_{0.5}[C_2A_2]_{0.5}$ are initially investigated to pre-screen potential ion identities of DSILs. Their infinite dilution capacity and selectivity on the mass basis are predicted by the COSMO-RS model as follows:

$$C_m^{\infty} = \left(1/\gamma_{\text{thiophene}}^{\infty}\right) \times \frac{MW_{\text{thiophee}}}{MW_{\text{DSIL}}} \tag{3}$$

$$S_m^{\infty} = \left(\gamma_{\text{octane}}^{\infty}/\gamma_{\text{thiophene}}^{\infty}\right) \times \frac{MW_{\text{thiophene}}}{MW_{\text{octane}}} \tag{4}$$

where $MW_{\text{thiophene}}$, MW_{DSIL}, and MW_{octane} refer to the molecular weight of thiophene, DSIL, and *n*-octane, respectively. It should be mentioned that the mole based C^{∞} and S^{∞} are used in Section 2 so that one can recognize the non-ideal 'mixing' properties of DSILs by avoiding the effect of molecular weights of ions involved in DSILs, and thus analyze the different tendencies of them from the molecular point of view. However, in our previous study,[16] the mass based C_m^{∞} and S_m^{∞} have been proven to be more efficient than the molar based C^{∞} and S^{∞} (see Eqs. 1 - 2) for quickly pre-screening promising IL solvents. The reason is that the molecular weights of ILs

usually vary in a large range and are generally much higher than those of conventional organic solvents, which also holds for DSILs screening. For a specific separation process, a commonly used organic solvent could be employed as a benchmark to filter out potential ion identities of DSILs.

QSPR based estimation of physical properties

For a practical extraction process, the melting point (T_m) and viscosity (η) of the solvent are important physical properties that need to be considered in addition to its extractive power. Since the study of DSILs is still in its infancy, there is no available quantitative structure-property relationship (QSPR) model that can be directly applied to evaluate T_m and η of them. However, according to previous reports, DSIL in many cases possesses a lower melting point than its IL parents, presenting as a eutectic 'mixture'.[32,37,50-52] Meanwhile, as indicated by Table S4 (Supporting Information), the viscosity of DSIL generally shows an acceptable deviation from the molar average viscosity of its IL parents (with a $\Delta\eta$ of 13.80 cP for 2471 data points involving DSILs with 47 different ion identities and ion ratios from 0 to 1).[38,53-55] Therefore, in the second step, T_m and η of the pre-screened DSILs from the first step are empirically estimated from those of their IL parents.

The T_m of the IL parents of DSILs is predicted by the group contribution model developed by Lazzús,[56]

$$T_m = 288.7 + \sum_{i=1}^{31} n_i \Delta t_{ci} + \sum_{j=1}^{36} n_j \Delta t_{aj} \quad (5)$$

where n_i and n_j are the numbers of cation group *i* and anion group *j* in ILs; Δt_{ci} and Δt_{aj} are the contributions of the cation and anion group to the T_m, respectively. This model is parameterized from the experimental T_m data of 400 different ILs covering 31 cation groups and 36 anion groups. The mean absolute percentage error (MAPE) between the experimental and estimated T_m is less than 7%. The viscosity of the IL parents of DSILs is calculated by a group contribution based feed-forward artificial neural network model.[57] This model is developed based on over 13000 data of temperature- and pressure-dependent viscosity of 1484 ILs, giving a MAPE of 11.1% and 13.8% for the training and testing dataset, respectively. In addition to the QSPR prediction, the T_m and η of some common ILs have already been experimentally reported and can be used instead. Admittedly, the estimations of the T_m and η of DSILs based on those of their IL parents may lead to inevitable deviations in some cases. In the long term, more experimental studies on the key physical properties of DSILs and reliable models thereon are of very high interest.

COSMO-RS based prediction of phase equilibrium behaviors

In the third step, the phase equilibrium properties of the DSILs retained from the first two steps are predicted by COSMO-RS. To begin with, the distribution coefficient (β) and selectivity (S) of the DSILs at the specific thiophene/*n*-octane mixture composition of interest are calculated as:

$$\beta = m^{E}_{\text{thiophene}} \Big/ m^{R}_{\text{thiophene}} \tag{6}$$

$$S = \frac{m^{E}_{\text{thiophene}}}{m^{R}_{\text{thiophene}}} \Bigg/ \frac{m^{E}_{\text{octane}}}{m^{R}_{\text{octane}}} \tag{7}$$

where $m_{thiophene}$ and m_{octane} refer to the mass fractions of thiophene and *n*-octane in the liquid-liquid equilibria (LLE) of the {DSILs + thiophene + *n*-octane} ternary systems; superscripts E and R represent the extract and the raffinate phase, respectively. Compared to the infinite dilution thermodynamic properties, the β and S derived from phase equilibrium have been demonstrated to be more rational for finding practically attractive solvents due to the consideration of the particular extraction conditions.[16]

The $[C_1]_{0.5}[C_2]_{0.5}A$, $C[A_1]_{0.5}[A_2]_{0.5}$, and $[C_1A_1]_{0.5}[C_2A_2]_{0.5}$ DSILs presenting high β and S are screened out for further optimization of the ion ratio *x*. Specifically, the LLE of {DSILs + thiophene + *n*-octane} for these DSILs with different *x* values are calculated under the same condition as stated above. The β and S are correspondingly calculated, and the optimal *x* or *x* range for each DSIL can thus be determined.

Experimental validation of practical extraction performances

From the above three model-based steps, promising DSIL candidates with specific ion identities and ion ratios are identified. However, it is highly desirable that the applicability of the solvents can be finally validated by experiments. Therefore, for the example of thiophene/*n*-octane separation, LLE experiments of {DSILs + thiophene + *n*-octane} were carried out. The ILs used for preparing the identified DSILs were purchased from the Monils Chem. Eng. Sci. & Tech. Co., Ltd. (Shanghai) with the purities higher than 98.5 wt%, which were confirmed by ^{1}H-NMR with an AVANCE III 400 MHz digital spectrometer (Bruker, Germany). Before use, these ILs were dried for 48 h under reduced pressure to remove possible volatile impurities and traces of water.

After drying, the water content in them was determined to be lower than 1000 ppm with an AQV-300 Karl-Fischer volumetric titration (Hiranuma, Japan). Thiophene and *n*-octane were supplied by Aladdin Chemical Co., Ltd. with purity above 99.0 wt%, and were used without further purification.

Before performing the LLE experiments, DSILs with different ion ratios were prepared by mixing a known amount of one of its parents with the other,[34,36,50] where the mass of each IL parent was gravimetrically measured by a Sartorius BSA224S-CW balance (Germany) with a precision of ±0.0001 g. After stirring for 3 h, the 'mixture' is visually inspected to make sure a homogenous DSIL is obtained. The prepared DSIL will be stored in a vacuum desiccator for further experiments. In a typical LLE, the DSIL (1), thiophene (2) and *n*-octane (3) were introduced successively into a screw-capped vial, where their masses (M_1, M_2, M_3) were determined gravimetrically. After tightly sealed, the mixture was continuously agitated with a magnetic stirrer for 3 h and then settled for 6 h to ensure complete thermodynamic equilibrium. The temperature of the liquid mixture was controlled by an oil bath with a temperature fluctuation of ±0.1 K (Huber Ministat 230, Germany). After settling, samples of the raffinate (R) and extract (E) phases were carefully withdrawn and analyzed by a gas chromatograph (Agilent 7890 GC, USA) equipped with a flame ionization detector and a PEG-20M column. The non-volatile DSILs were collected in a pre-column (5 m × 0.250 mm, uncoated fused silica) in order not to disrupt the analysis. An internal standard method was applied to determine the mass ratio of thiophene-to-octane in both phases, i.e., m_{2R}/m_{3R} and m_{2E}/m_{3E}. The concentration of DSIL in

the raffinate phase (m_{1R}) was analyzed by the nitrogen content, which can be determined precisely with a chemiluminescence nitrogen analyzer (Antek 9000, USA). The detection range of the nitrogen analyzer is 20 ppb - 17% and different standard calibration lines can be employed at each small interval within the range to ensure the accuracy of analysis. In summary, the LLE compositions of both phases can be finally determined by combining the overall mass balance, the GC analysis results, and the concentration of DSIL in the raffinate phase.

Method application to the thiophene/*n*-octane separation

Step 1: Pre-screening of DSILs based on C_m^∞ and S_m^∞

For the separation of thiophene and *n*-octane, sulfolane is used as benchmark solvent for DSILs pre-screening because it is regarded as one of the most efficient conventional solvents for this process.[16,25,58] In the first step, 44 $[C_1]_{0.5}[C_2]_{0.5}A$, 139 $C[A_1]_{0.5}[A_2]_{0.5}$, and 33 $[C_1A_1]_{0.5}[C_2A_2]_{0.5}$ of the initially covered ion identities of DSILs are recognized with higher C_m^∞ and S_m^∞ than those of sulfolane (C_m^∞=0.49, S_m^∞=17.68); in contrast, only 14 two-ion ILs are retained based on the same requirement (see Figure 5). The pre-screened 216 ion identities of DSILs and 14 ILs are listed in Table S5 (Supporting Information). The much larger number of satisfying DSILs clearly demonstrates that DSILs provide more opportunities to find promising solvents for this separation process. For instance, both the C_m^∞ and S_m^∞ of the DSIL $[C_2MPy][BF_4]_{0.5}[OAc]_{0.5}$ (C_m^∞=0.65, S_m^∞=41.22) are notably higher than those of sulfolane, whereas neither [C_2MPy][OAc]

(C_m^{∞} =1.06, S_m^{∞} =12.72) nor [C_2MPy][BF_4] (C_m^{∞} =0.37, S_m^{∞} =186.86) can meet the two requirements simultaneously. It is worth mentioning that more ion identities of DSILs, even some more promising ones (as indicated in Figure 3), can be found if different ion ratios are taken into account in this step. Nevertheless, for the sake of computational cost, only the satisfying ion identities of DSILs at the ion ratio of 0.5 are further considered in the following steps.

Step 2: Further screening based on T_m and η

To further screen promising solvent candidates, the upper bound of the T_m of DSILs is set to 298.15 K. For this purpose, the T_m for one of the IL parents of DSILs is constrained to be lower than 298.15 K and for the other is limited to be below 323.15 K. 4 $[C_1]_{0.5}[C_2]_{0.5}A$, 45 $C[A_1]_{0.5}[A_2]_{0.5}$, and 21 $[C_1A_1]_{0.5}[C_2A_2]_{0.5}$ of the DSILs pre-screened from Step 1 satisfy the T_m constraint, while only 2 two-ion ILs are retained (see Table S6, Supporting Information). Following this, the η for one of the IL parents of DSILs is confined below 100 cP and for the other is confined below 200 cP at 298.15 K in order to ensure that the selected DSILs have relatively low viscosity. Through such η constraints, 23 $C[A_1]_{0.5}[A_2]_{0.5}$ and 11 $[C_1A_1]_{0.5}[C_2A_2]_{0.5}$ are further preserved while only 1 two-ion IL [C_2MIm][OPr] survives (see Table S7, Supporting Information). Of course, the above empirical limitations on T_m and η can be properly relaxed if more DSILs are desired for further evaluation.

Figure 6 compares the C_m^∞ and S_m^∞ of the DSILs and two-ion ILs screened after taking account of the T_m and η constraints. As shown, all the selected DSILs have higher C_m^∞ and/or S_m^∞ than the survived IL [C_2MIm][OPr], indicating their higher potential for the thiophene/*n*-octane separation. This comparison demonstrates that DSILs open access to more attractive solvents compared to two-ion ILs. As highlighted in Figure 6, 5 ion identities of DSILs can be connected to form a pseudo Pareto front and no DSILs below this front can overwhelm them from both C_m^∞ and S_m^∞. Among them, only [C_2MIm][OAc]$_{0.5}$[SCN]$_{0.5}$, [C_2MPy][OAc]$_{0.5}$[SCN]$_{0.5}$, and [C_2MIm][OAc]$_{0.5}$[NO_3]$_{0.5}$ are further considered in the subsequent steps since they can achieve a better trade-off between C_m^∞ and S_m^∞.

Step 3: Further screening based on phase equilibrium properties

From the practical point of view, the separation of a low concentration of thiophene from *n*-octane is more interesting since it could simulate the deep extractive desulfurization process of fuel oils. Therefore, the LLE of {DSILs + thiophene + *n*-octane} in the low thiophene concentration range are calculated to better evaluate the separation performances of the 3 DSILs retained after Step 2. As depicted in Figure 7, the LLE-derived β and S of them are all much higher than those of sulfolane in the studied concentration range, indicating that they are more promising solvents for the thiophene/*n*-octane separation. To be specific, their β follow the ranking of [C_2MIm][OAc]$_{0.5}$[NO_3]$_{0.5}$ > [C_2MPy][OAc]$_{0.5}$[SCN]$_{0.5}$ > [C_2MIm][OAc]$_{0.5}$[SCN]$_{0.5}$ > sulfolane. Meanwhile, their S are in the ranking of [C_2MIm][OAc]$_{0.5}$[SCN]$_{0.5}$ >

$[C_2MPy][OAc]_{0.5}[SCN]_{0.5}$ ≈ $[C_2MIm][OAc]_{0.5}[NO_3]_{0.5}$ > sulfolane, where the S of $[C_2MIm][OAc]_{0.5}[NO_3]_{0.5}$ is very close to that of $[C_2MPy][OAc]_{0.5}[SCN]_{0.5}$ with the thiophene concentration below 0.01 and afterwards becomes slightly higher. The difference between the LLE-derived S and the S_m^∞ results (see Figure 6) verifies the importance of estimating the extraction performances of DSILs at practical conditions. Overall, $[C_2MIm][OAc]_{0.5}[NO_3]_{0.5}$ and $[C_2MIm][OAc]_{0.5}[SCN]_{0.5}$ are further considered because of the highest β and S in the low thiophene concentration range, respectively.

For the selected ion identities of DSILs, i.e., $[C_2MIm][OAc]_x[NO_3]_{1-x}$ and $[C_2MIm][OAc]_x[SCN]_{1-x}$, the LLE of {DSILs + thiophene + *n*-octane} with different *x* are calculated at a fixed global composition of [0.500, 0.005, 0.495] on the mass basis, and the corresponding β and S are determined. As seen in Figure 8, their β grow whereas their S decline gradually with *x* of the DSILs increasing from 0 to 1. The monotonic increase of β for $[C_2MIm][OAc]_x[NO_3]_{1-x}$ and $[C_2MIm][OAc]_x[SCN]_{1-x}$ corresponds well to the predictions on their C^∞, demonstrating that they belong to the Group 1 in Figure 3 (see Table S3, Supporting Information). Furthermore, in order to ensure that the DSILs have higher β and S than sulfolane at the same extraction condition, the feasible *x* range is [0, 1] for $[C_2MIm][OAc]_x[NO_3]_{1-x}$ and [0.30, 1] for $[C_2MIm][OAc]_x[SCN]_{1-x}$ (see Figure 8). Such *x* ranges for the two DSILs will be validated experimentally in the next step.

Step 4: Final identification by LLE experiments

From above, $[C_2MIm][OAc]_x[NO_3]_{1-x}$ with x of [0, 1] and $[C_2MIm][OAc]_x[SCN]_{1-x}$ with x of [0.30, 1] are screened out as promising DSILs for thiophene/*n*-octane separation. Before experimentally validating the extraction performances of such DSILs, they are prepared accordingly by the addition of $[C_2MIm][OAc]$ into $[C_2MIm][NO_3]$ and into $[C_2MIm][SCN]$, respectively. At 298.15 K, a clear homogenous 'mixture' is observed for $[C_2MIm][OAc]$ and $[C_2MIm][NO_3]$ in the whole x range, whereas for $[C_2MIm][OAc]$ and $[C_2MIm][SCN]$, the 'mixture' becomes cloudy with x below 0.70. That is to say, only DSILs of $[C_2MIm][OAc]_x[NO_3]_{1-x}$ (x=[0, 1]) and $[C_2MIm][OAc]_x[SCN]_{1-x}$ (x=[0.70, 1]) are available for experimental validation.

After preparing the DSILs, the LLE experiments of {DSILs + thiophene + *n*-octane} are performed at the same global composition of [0.500, 0.005, 0.495] on the mass basis. The obtained LLE compositions are listed in Table S8 (Supporting Information) together with the corresponding COSMO-RS predictions. The root mean square deviations (RMSD) between them are calculated as:

$$RMSD = \left\{ \sum_i \sum_l \sum_k \left(m_{ilk}^{\exp} - m_{ilk}^{cal} \right)^2 / 6n \right\}^{1/2} \quad (8)$$

where m is the component mass fraction; the subscripts i, l, and k represent the component, the phase, and the tie-line, respectively; n denotes the total number of tie-lines (obtained at different x values of DSILs). For the ternary systems based on $[C_2MIm][OAc]_x[NO_3]_{1-x}$ (x=[0, 1]) and

$[C_2MIm][OAc]_x[SCN]_{1-x}$ (x=[0.7, 1]), the estimated RMSDs are 0.0178 and 0.0210, respectively, which demonstrate the acceptable accuracy of COSMO-RS predictions for the studied DSIL systems. Figure 9 shows the β and S derived from the experimental LLE as a function of x. As seen, the β of $[C_2MIm][OAc]_x[NO_3]_{1-x}$ gradually increases from 0.58 at x=0 (i.e., $[C_2MIm][NO_3]$) to 0.74 at x=1 (i.e., $[C_2MIm][OAc]$), while the S decreases from 305.87 to 138.77 along the x axis. For $[C_2MIm][OAc]_x[SCN]_{1-x}$, the increasing of β from 0.64 to 0.74 and the decreasing of S from 258.00 to 138.78 are also observed as x increases from 0.70 to 1. Compared with Figure 8, COSMO-RS overestimates the β of $[C_2MIm][OAc]_x[NO_3]_{1-x}$ (x=[0, 1]) and $[C_2MIm][OAc]_x[SCN]_{1-x}$ (x=[0.7, 1]) due to a higher prediction of the very low thiophene concentration in the extract phase (see Table S8, Supporting Information). Nevertheless, the dependencies of β and S of DSILs on x are well captured, which validates the suitability of COSMO-RS for DSILs screening. Moreover, comparing to the recently reported ILs for similar separation systems, the S of the identified DSILs are much higher and their β are also satisfying, indicating their great potential for the thiophene/*n*-octane separation.[16,59]

Conclusions

In this work, a multilevel DSILs design method is proposed and applied to select extraction solvents for the thiophene/*n*-octane separation. From the basis set of 20 cations and 25 anions, $[C_2MIm][OAc]_x[NO_3]_{1-x}$ (x=[0, 1]) and $[C_2MIm][OAc]_x[SCN]_{1-x}$ (x=[0.70, 1]) are identified as promising DSILs, which are shown to be more attractive compared to the correspondingly

screened two-ion ILs. The experimental liquid-liquid equilibria of {DSILs + thiophene + *n*-octane} demonstrate the high extraction performances of the selected DSILs, which validate the reliability of the proposed method.

The concept of DSILs opens access to another way of designing IL-type solvents for specific applications, by choosing not only the ion identity but also the ion ratio. Due to the fact that the proposed DSIL design method can be easily adapted to other separation systems, we believe it can play an essential role in the development of DSIL-based separation processes.

Acknowledgments

Zhen Song acknowledges the support of Max Planck Society for his Postdoc program in the Max Planck Institute for Dynamics of Complex Technical Systems, Magdeburg, Germany. Moreover, this research is supported by the Natural Science Foundation of China (21776074 and 21406063).

References

1. Brennecke JF, Maginn, EJ. Ionic liquids: innovative fluids for chemical processing. *AIChE J.* 2001;47(11):2384-2389.
2. Ventura, SP, e Silva FA, Quental MV, Mondal, D, Freire MG, Coutinho JA. Ionic-liquid-mediated extraction and separation processes for bioactive compounds: past, present, and future trends. *Chem. Rev.* 2017;117(10):6984-7052.
3. Zeng S, Zhang X, Bai L, Zhang X, Wang H, Wang J, Bao D, Li M, Liu X, Zhang, S. Ionic-liquid-based CO_2 capture systems: structure, interaction and process. *Chem. Rev.* 2017;117(14):9625-9673.

4. Bedia J, Ruiz E, Riva J, Ferro VR, Palomar J, Rodriguez J. Optimized ionic liquids for toluene absorption. *AIChE J*. 2013;59(5):1648-1656.
5. Alvarez-Guerra E, Irabien A, Ventura SP, Coutinho JA. Ionic liquid recovery alternatives in ionic liquid-based three-phase partitioning (ILTPP). *AIChE J*. 2014;*60*(10):3577-3586.
6. Song Z, Zhang J, Zeng Q, Cheng H, Chen L, Qi Z. Effect of cation alkyl chain length on liquid-liquid equilibria of {ionic liquids+ thiophene+ heptane}: COSMO-RS prediction and experimental verification. *Fluid Phase Equilibr.* 2016;425:244-251.
7. e Silva FA, Caban M, Stepnowski P, Coutinho JA, Ventura SP. Recovery of ibuprofen from pharmaceutical wastes using ionic liquids. *Green Chem*. 2016;18(13):3749-3757.
8. Dong Y, Dai C, Lei Z. Extractive distillation of methylal/methanol mixture using the mixture of dimethylformamide (DMF) and ionic liquid as entrainers. *Fuel*. 2018;*216*:503-512.
9. Han J, Dai C, Lei ZG, Chen B. Gas drying with ionic liquids. *AIChE J*. 2018;*64*(2):606-619.
10. Wang X, Zeng S, Wang J, Shang D, Zhang XP, Liu J, Zhang Y. Selective separation of hydrogen sulfide with pyridinium-based ionic liquids. *Ind Eng Chem Res.* 2018;57(4):1284-1293.Kulajanpeng K, Suriyapraphadilok U, Gani R. Systematic screening methodology and energy efficient design of ionic liquid-based separation processes. *J Clean Prod.* 2016;*111:*93-107.

11. Song Z, Zhou T, Zhang J, Cheng H, Chen L, Qi Z. Screening of ionic liquids for solvent-sensitive extraction–with deep desulfurization as an example. *Chem Eng Sci*. 2015;*129*:69-77.
12. Zhao X, Yang Q, Xu D, Bao Z, Zhang Y, Su B, Ren Q, Xing H. Design and screening of ionic liquids for C_2H_2/C_2H_4 separation by COSMO-RS and experiments. *AIChE J*. 2015;*61*(6):2016-2027.
13. Liu X, Huang Y, Zhao Y, Gani R, Zhang XP, Zhang S. Ionic liquid design and process simulation for decarbonization of shale gas. *Ind Eng Chem Res*. 2016; *55*(20): 5931-5944.
14. Kunov-Kruse AJ, Weber C, Rogers RD, Myerson AS. The a priori design and selection of ionic liquids as solvents for active pharmaceutical ingredients. *Chem Eur J*. 2017;23(23):5498-5508.
15. Song Z, Zhou T, Qi Z, Sundmacher K. Systematic method for screening ionic liquids as extraction solvents exemplified by an extractive desulfurization process. *ACS Sustain Chem Eng*. 2017;*5*(4):3382-3389.
16. de Riva J, Suarez-Reyes J, Moreno D, Díaz I, Ferro V, Palomar J. Ionic liquids for post-combustion CO_2 capture by physical absorption: thermodynamic, kinetic and process analysis. *Int J Greenh Gas Con*. 2017;61:61-70.
17. Zhao Y, Gani R, Afzal RM, Zhang XP, Zhang SJ. Ionic liquids for absorption and separation of gases: an extensive database and a systematic screening method. *AIChE J*. 2017;*63*(4):1353-1367.

18. Yu G, Dai C, Wu L, Lei ZG. Natural gas dehydration with ionic liquids. *Energy Fuels.* 2017;*31*(2):1429-1439.

19. Roughton BC, Christian B, White J, Camarda KV, Gani R. Simultaneous design of ionic liquid entrainers and energy efficient azeotropic separation processes. *Comput Chem Eng*. 2012;42:248-262.

20. Lei ZG, Dai C, Wang W, Chen B. UNIFAC model for ionic liquid-CO_2 systems. *AIChE J*. 2014;60(2):716-729.

21. Lei ZG, Dai, C, Yang Q, Zhu J, Chen B. UNIFAC model for ionic liquid-$CO(H_2)$ systems: An experimental and modeling study on gas solubility. *AIChE J*. 2014;60(12): 4222-4231.

22. Chong FK, Andiappan V, Ng DK, Foo DC, Eljack F, Atilhan M, Chemmangattuvalappil NG. Design of ionic liquid as carbon capture solvent for a bioenergy system: integration of bioenergy and carbon capture systems. *ACS Sustain Chem Eng*. 2017;*5*(6):5241-5252.

23. Chao H, Song Z, Cheng H, Chen L, Qi Z. Computer-aided design and process evaluation of ionic liquids for n-hexane-methylcyclopentane extractive distillation. *Sep Purif Technol*. 2018;196:157-165.

24. Song Z, Zhang C, Qi Z, Zhou T, Sundmacher K. Computer-aided design of ionic liquids as solvents for extractive desulfurization. *AIChE J*. 2018;64(3):1013-1025.Ng LY, Chong FK, Chemmangattuvalappil NG. Challenges and opportunities in computer-aided molecular design. *Comput Chem Eng.* 2015;*81*:115-129.García S, Larriba M, García J, Torrecilla JS, Rodríguez F. Separation of toluene from n-heptane by liquid–liquid extraction using binary

mixtures of [bpy][BF_4] and [4bmpy][Tf_2N] ionic liquids as solvent. *J Chem. Thermodyn*. 2012;53:119-124.

25. Lei ZG, Han J, Zhang B, Li Q, Zhu J, Chen B. Solubility of CO_2 in binary mixtures of room-temperature ionic liquids at high pressures. *J Chem Eng Data*. 2012;57(8):2153-2159.
26. Potdar S, Anantharaj R, Banerjee T. Aromatic extraction using mixed ionic liquids: experiments and COSMO-RS predictions. *J Chem Eng Data*. 2012;57(4):1026-1035.Pinto AM, Rodríguez H, Colón YJ, Arce Jr A, Arce A, Soto A. Absorption of carbon dioxide in two binary mixtures of ionic liquids. *Ind Eng Chem Res.* 2013;52:5975-5984.
27. Lee BS, Lin ST. Prediction and screening of solubility of pharmaceuticals in single- and mixed-ionic liquids using COSMO-SAC model. *AIChE J*. 2017;63(7):3096-3104.
28. Niedermeyer H, Hallett JP, Villar-Garcia IJ, Hunt PA, Welton T. Mixtures of ionic liquids. *Chem Soc Rev*. 2012;41(23):7780-7802.
29. Larriba M, Navarro P, Delgado-Mellado N, González C, García J, Rodríguez F. Dearomatization of pyrolysis gasoline with an ionic liquid mixture: Experimental study and process simulation. *AIChE J*. 2017;63(9):4054-4065.
30. Pereira JF, Barber PS, Kelley, SP, Berton P, Rogers RD. Double salt ionic liquids based on 1-ethyl-3-methylimidazolium acetate and hydroxyl-functionalized ammonium acetates: strong effects of weak interactions. *Phys Chem Chem Phys*. 2017;19(39): 26934-26943.

31. Atilhan M, Anaya B, Ullah R, Costa LT, Aparicio S. Double salt ionic liquids based on ammonium cations and their application for CO_2 capture. *J Phys Chem C*. 2016;120(31):17829-17844.
32. Wang H, Berton P, Myerson AS, Rogers RD. Double salt ionic liquids containing the trihexyl(tetradecyl)phosphonium cation: the ability to tune the solubility of aromatics, ethers, and lipophilic compounds. *ECS Trans*. 2016;75(15):451-65.
33. Chatel G, Pereira JF, Debbeti V, Wang H, Rogers RD. Mixing ionic liquids - "simple mixtures" or "double salts"? *Green Chem*. 2014;16(4):2051-2083.
34. Clough MT, Crick CR, Gräsvik J, Hunt PA, Niedermeyer H, Welton T, Whitaker OP. A physicochemical investigation of ionic liquid mixtures. *Chem Sci*. 2015;6(2):1101-1114.
35. Matthews RP, Villar-Garcia IJ, Weber C, Griffith J, Cameron F, Hallett JP, Hunt P, Welton T. A structural investigation of ionic liquid mixtures. *Phys Chem Chem Phys*. 2016;18(12):8608-8624.
36. Moya C, Gonzalez-Miquel M, Rodriguez F, Soto A, Rodriguez H, Palomar J. Non-ideal behavior of ionic liquid mixtures to enhance CO_2 capture. *Fluid Phase Equilibr.* 2017;*450*:175-183.Eckert F, Klamt A. Fast solvent screening via quantum chemistry: COSMO-RS approach. *AIChE J*. 2002;48(2):369-385.
37. Banerjee T, Khanna A. Infinite dilution activity coefficients for trihexyltetradecyl phosphonium ionic liquids: measurements and COSMO-RS prediction. *J Chem Eng Data*. 2006;51(6):2170-2177.

38. Zhou T, Chen L, Ye Y, Chen L, Qi Z, Freund H, Sundmacher K. An overview of mutual solubility of ionic liquids and water predicted by COSMO-RS. *Ind Eng Chem Res.* 2012;51(17):6256-6264.

39. Ferreira AR, Freire MG, Ribeiro JC, Lopes FM, Crespo JG, Coutinho JA. Overview of the liquid–liquid equilibria of ternary systems composed of ionic liquid and aromatic and aliphatic hydrocarbons, and their modeling by COSMO-RS. *Ind Eng Chem Res.* 2012;51(8):3483-3507.

40. Kurnia KA, Coutinho JA. Overview of the excess enthalpies of the binary mixtures composed of molecular solvents and ionic liquids and their modeling using COSMO-RS. *Ind Eng Chem Res*. 2013;52(38):13862-13874.

41. Song Z, Zeng Q, Zhang J, Cheng H, Chen L, Qi ZW. Solubility of imidazolium-based ionic liquids in model fuel hydrocarbons: A COSMO-RS and experimental study. *J Mol Liq*. 2016;224:544-550.

42. Matheswaran P, Wilfred CD, Kurnia KA, Ramli A. Overview of activity coefficient of thiophene at infinite dilution in ionic liquids and their modeling using COSMO-RS. *Ind Eng Chem Res*. 2016;55(3):788-797.

43. Paduszyński K. An overview of the performance of the COSMO-RS approach in predicting the activity coefficients of molecular solutes in ionic liquids and derived properties at infinite dilution. *Phys Chem Chem Phys.* 2017;19:11835-11850.

44. Omar S, Lemus J, Ruiz E, Ferro VR, Orteg, J, Palomar J. Ionic liquid mixtures-an analysis of their mutual miscibility. *J Phys Chem B.* 2014;118(9):2442-2450.

45. Annat G, Forsyth M, MacFarlane DR. Ionic liquid mixtures - variations in physical properties and their origins in molecular structure. *J Phys Chem B.* 2012;116:8251-8258.

46. Smiglak M, Bridges NJ, Dilip M, Rogers RD. Direct, atom efficient, and halide-free syntheses of azolium azolate energetic ionic liquids and their eutectic mixtures, and method for determining eutectic composition. *Chem Eur J.* 2008;*14*:11314-11319.

47. Fernandez L, Silva LP, Martins MA, Ferreira O, Ortega J, Pinho SP, Coutinho JA. Indirect assessment of the fusion properties of choline chloride from solid-liquid equilibria data. *Fluid Phase Equilibr*. 2017;*448*:9-14.

48. Larriba M, Navarro P, Beigbeder JB, García J, Rodríguez F. Mixing and decomposition behavior of {[4bmpy][Tf2N]+[emim][EtSO4]} and {[4bmpy][Tf2N]+[emim][TFES]} ionic liquid mixtures. *J Chem Thermodyn.* 2015;*82*:58-75.

49. Almeida HF, Canongia Lopes JN, Rebelo LP, Coutinho JA, Freire MG, Marrucho IM. Densities and viscosities of mixtures of two ionic liquids containing a common cation. *Journal of Chemical & Engineering Data* 2016;*61*:2828-2843.

50. Fillion J, Brennecke JF. Viscosity of ionic liquid–ionic liquid mixtures. *J Chem Eng Data*. 2017;62(6):1884-1901.

51. Lazzús JA. A group contribution method to predict the melting point of ionic liquids. *Fluid Phase Equilibria*. 2012;313:1-6.

52. Paduszyński K, Domańska U. Viscosity of ionic liquids: an extensive database and a new group contribution model based on a feed-forward artificial neural network. *J Chem Inf Model*. 2014;54(5):1311-1324.
53. Hansmeier AR, Meindersma GW, de Haan AB. Desulfurization and denitrogenation of gasoline and diesel fuels by means of ionic liquids. *Green Chem*. 2011;13(7):1907–1913.
54. Mafi M, Dehghani MR, Mokhtarani B. Novel liquid–liquid equilibrium data for six ternary systems containing IL, hydrocarbon and thiophene at 25° C. *Fluid Phase Equilibr*. 2016;*412*:21-28.

Table 1.

Classification of DSILs based on the different dependencies of their C^{∞} on the ion ratio *x*.

Groups	Number of DSILs		
	$[C_1]_x[C_2]_{1-x}A$	$C[A_1]_x[A_2]_{1-x}$	$[C_1A_1]_x[C_2A_2]_{1-x}$
Group 1	4314	5025	6706
Group 2	416	939	1773
Group 3	20	36	71

List of Figure Captions

Figure 1. C^{∞} (blue column) and S^{∞} (red column) of $[C_4MIm]_{0.5}[Cation]_{0.5}[BF_4]$ calculated by COSMO-RS.

Figure 2. C^{∞} (blue column) and S^{∞} (red column) of $[C_4MIm][BF_4]_{0.5}[Anion]_{0.5}$ calculated by COSMO-RS.

Figure 3. C^{∞} and S^{∞} of the representative DSILs of each group as a function of the ion ratio *x*.

Figure 4. Scheme of the proposed DSILs design method.

Figure 5. Prescreened ion identities of DSILs and two-ion ILs by applying the C_m^{∞} and S_m^{∞} constraints (sulfolane as the benchmark solvent).

Figure 6. Further screened ion identities of DSILs and two-ion ILs by applying the T_m and η constraints.

Figure 7. COSMO-RS predicted β and S of the DSILs screened after Step 2 as a function of the thiophene concentration in the raffinate phase (in comparison to sulfolane).

Figure 8. COSMO-RS predicted β and S of $[C_2MIm][OAc]_x[NO_3]_{1-x}$ and $[C_2MIm][OAc]_x[SCN]_{1-x}$ as a function of *x* at a mass-based global composition of [0.5, 0.005, 0.495] for {DSIL + thiophene + *n*-octane}.

Figure 9. Experimentally determined β and S of $[C_2MIm][OAc]_x[NO_3]_{1-x}$ (a) and $[C_2MIm][OAc]_x[SCN]_{1-x}$ (b) at a mass-based global composition of [0.5, 0.005, 0.495] for {DSIL + thiophene + *n*-octane}.

Figure 1. C^{∞} (blue column) and S^{∞} (red column) of $[C_4MIm]_{0.5}[Cation]_{0.5}[BF_4]$ calculated by COSMO-RS.

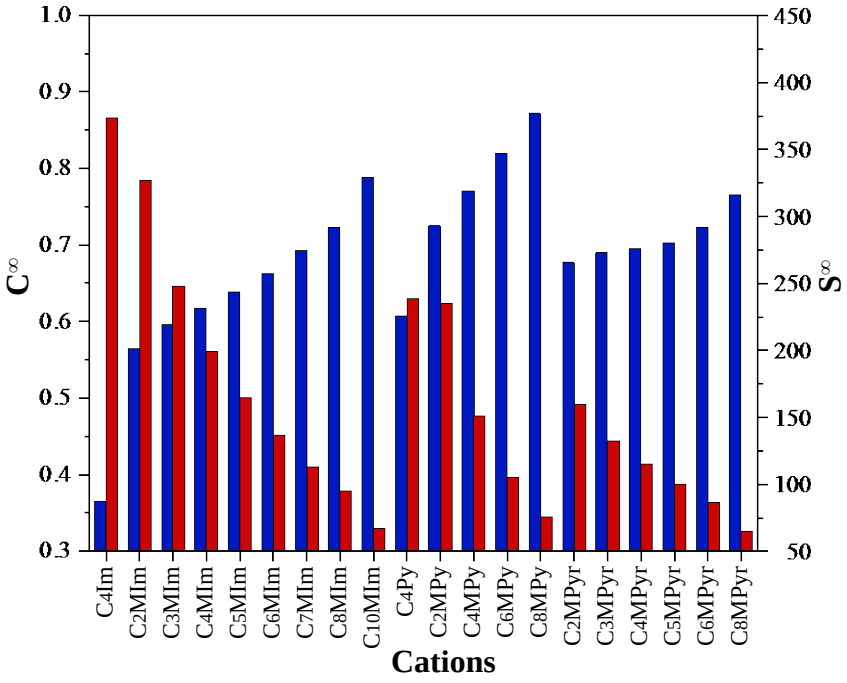

Figure 2. C^{∞} (blue column) and S^{∞} (red column) of $[C_4MIm][BF_4]_{0.5}[Anion]_{0.5}$ calculated by COSMO-RS.

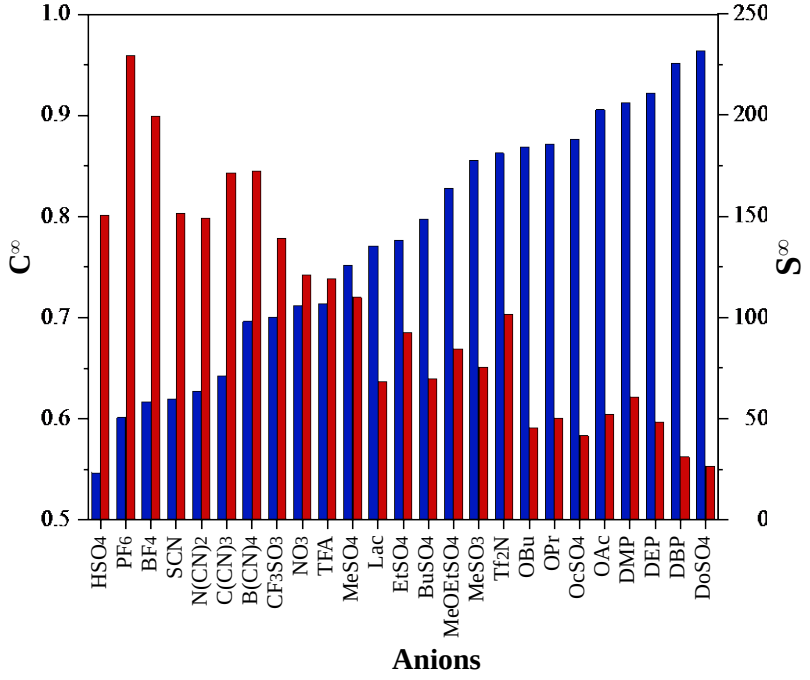

Figure 3. C^{∞} and S^{∞} of the representative DSILs of each group as a function of the ion ratio *x*.

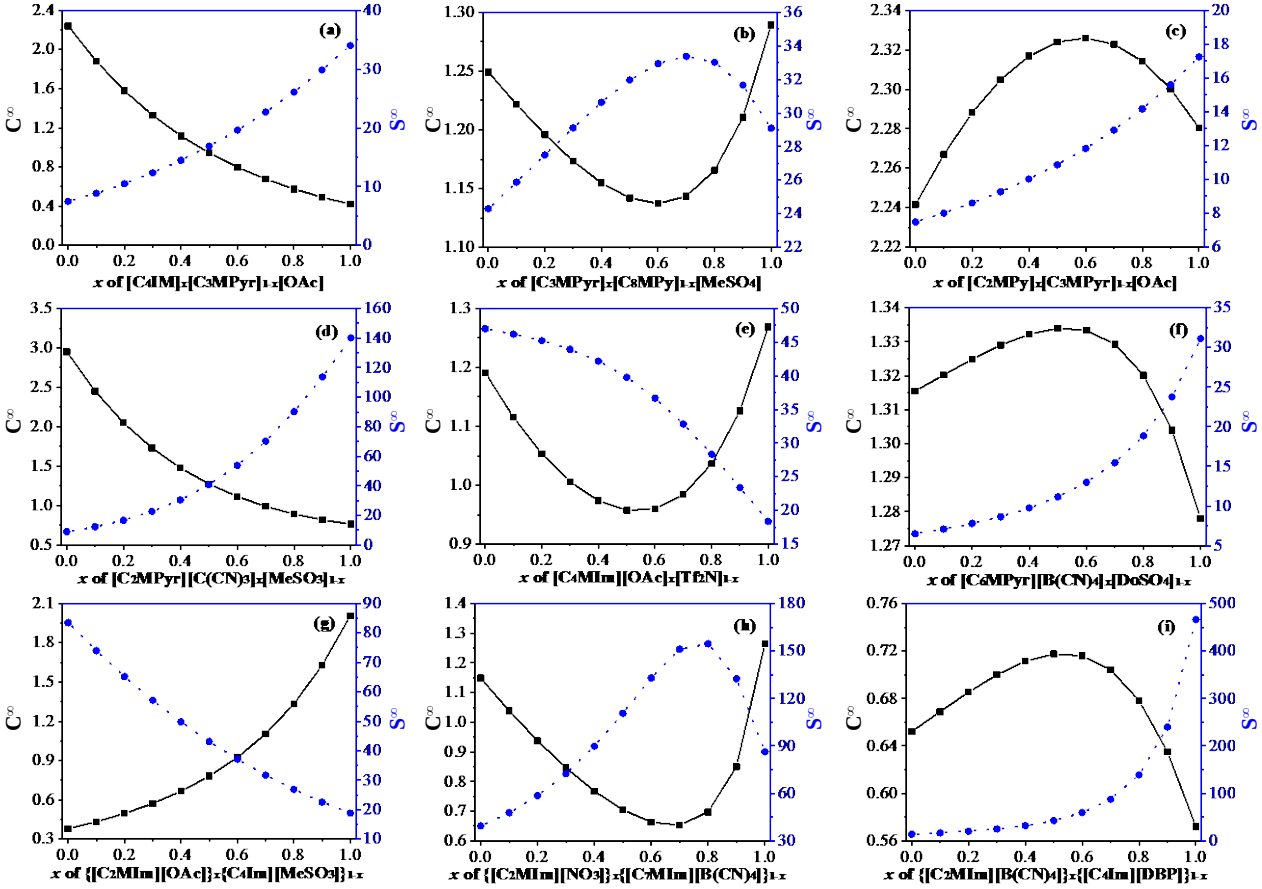

Group 1 **Group 2** **Group 3**

Figure 4. Scheme of the proposed DSILs design method.

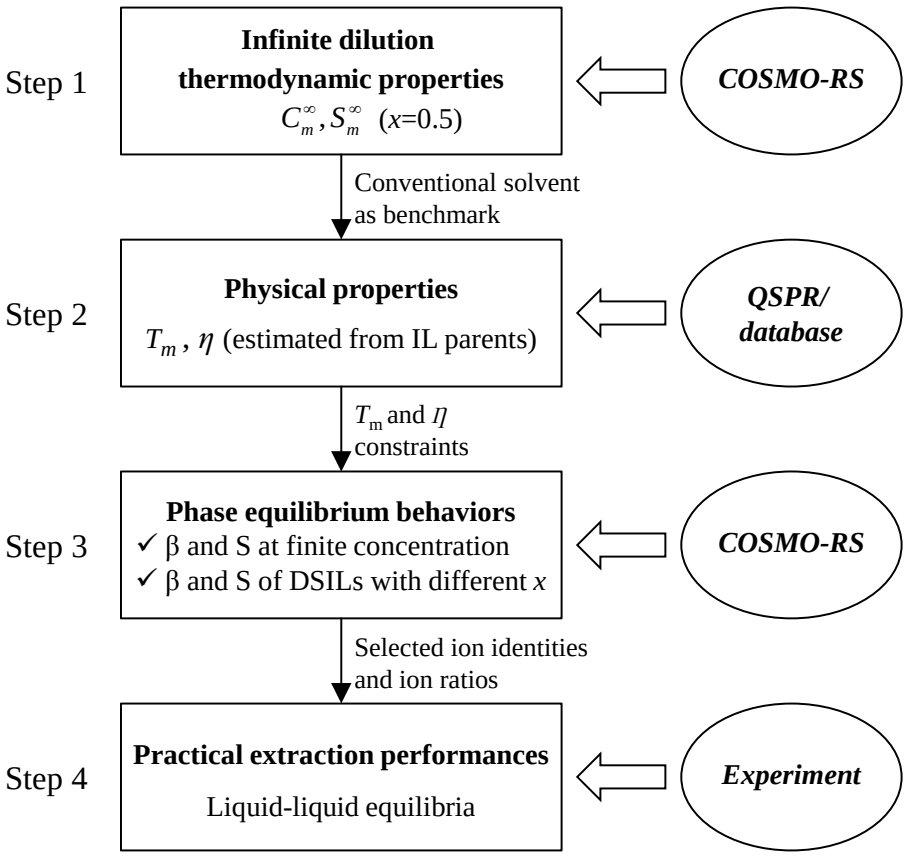

Figure 5. Prescreened ion identities of DSILs and two-ion ILs by applying the C_m^∞ and S_m^∞ constraints (sulfolane as the benchmark solvent).

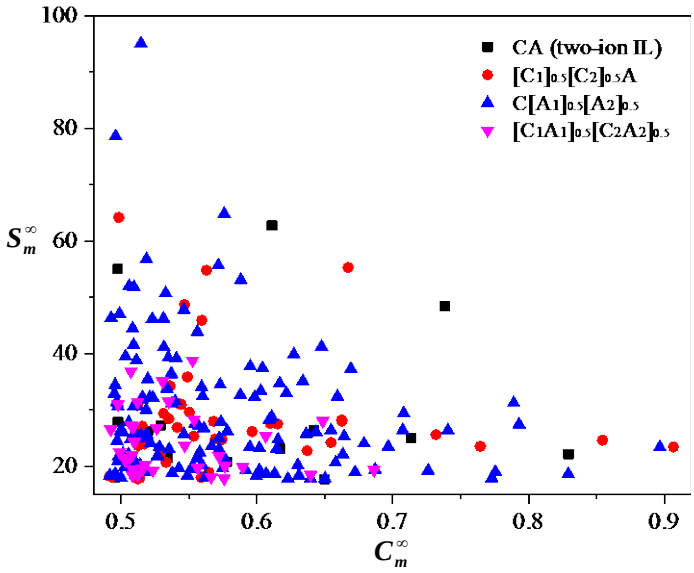

Figure 6. Further screened ion identities of DSILs and two-ion ILs by applying the T_m and η constraints.

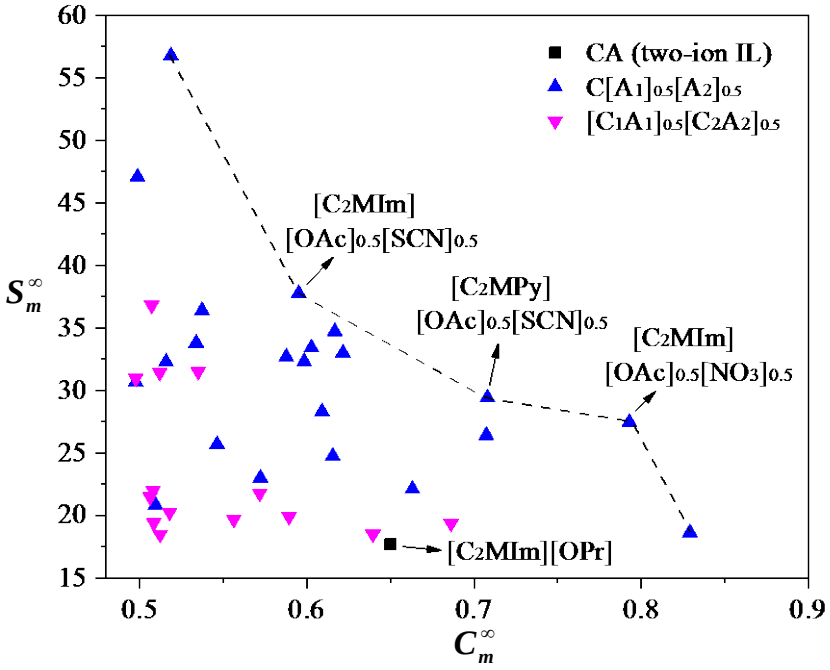

Figure 7. COSMO-RS predicted β and S of the DSILs screened after Step 2 as a function of the thiophene concentration in the raffinate phase (in comparison to sulfolane).

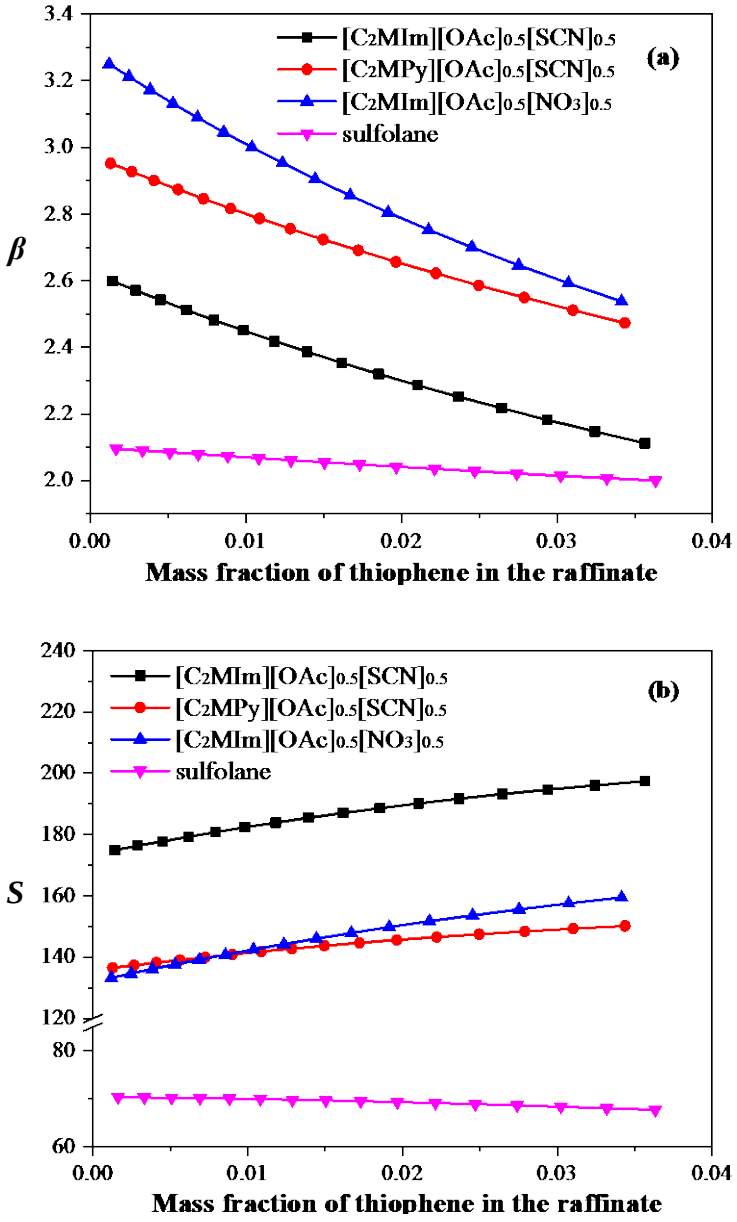

Figure 8. COSMO-RS predicted β and S of $[C_2MIm][OAc]_x[NO_3]_{1-x}$ and $[C_2MIm][OAc]_x[SCN]_{1-x}$ as a function of *x* at a mass-based global composition of [0.5, 0.005, 0.495] for {DSIL + thiophene + *n*-octane}.

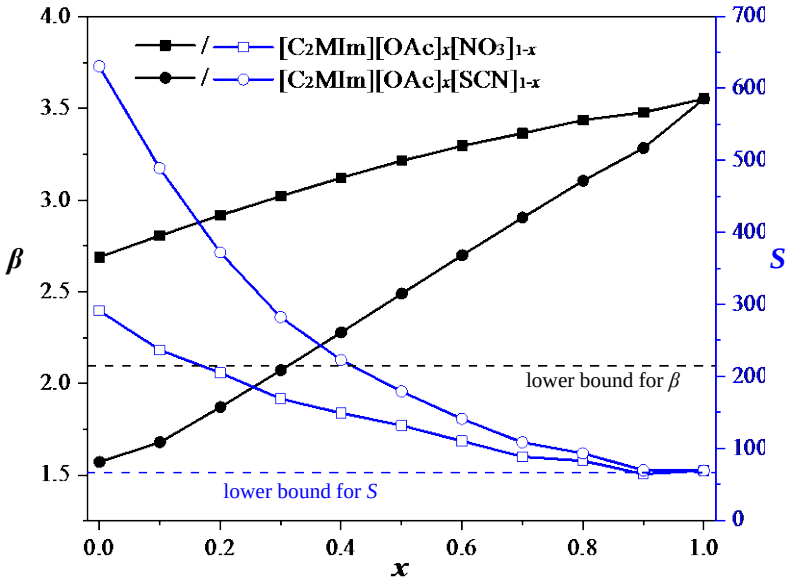

Figure 9. Experimentally determined β and S of $[C_2MIm][OAc]_x[NO_3]_{1-x}$ (a) and $[C_2MIm][OAc]_x[SCN]_{1-x}$ (b) at a mass-based global composition of [0.5, 0.005, 0.495] for {DSIL + thiophene + *n*-octane}.